ACS APPLIED MATERIALS & INTERFACES

www.acsami.org

Research Article

Electrochemical Trans-Channel Assay for Efficient Evaluation of Tumor Cell Invasiveness

Liu Shi, Lin Wang, Xuemei Ma, Mohammed Jalalah, Saeed A. Alsareii, Tao Gao,* Farid A. Harraz,* and Genxi Li*

Cite This: *ACS Appl. Mater. Interfaces* 2021, 13, 17268–17275

Read Online

ACCESS | Metrics & More | Article Recommendations | Supporting Information

ABSTRACT: Efficiently assessing the invasive capability of tumor cells is critical both for the research and treatment of cancer. Here, we report a novel method called the electrochemical trans-channel assay for efficient evaluation of tumor cell invasiveness. A bioinspired extracellular matrix degradation model (EDM) has been first fabricated on a porous anodic alumina (PAA) membrane to construct the electrochemical apparatus. Upon contacting the invasive tumor cells, invasive capability can be sensitively evaluated by the degree of EDM impairment, which is recorded by the electrochemical trans-channel ionic currents in a label-free manner. Compared to the most commonly used trans-well migration method, this assay can be accomplished in an efficient way that is significantly faster (20 min) and more convenient. Besides, quantitation can also be realized for monitoring the invasion process, which cannot be achieved by other currently used methods. Our proposed electrochemical trans-channel assay method has shown a synergistic effect for the evaluation of tumor cell invasiveness, providing a promising method for clinical assessment or prognostic applications of tumor metastasis.

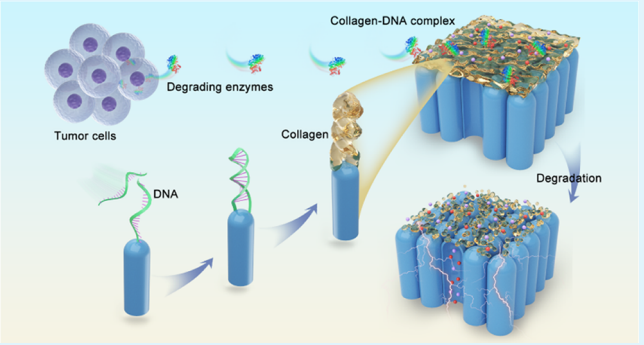

KEYWORDS: *electrochemical biosensor, nanochannels, tumor metastasis, extracellular matrix, trans-well migration assay*

1. INTRODUCTION

Invasion cascade, the spread of tumor cells from the primary site to distant sites, has been proven to be the principal cause of death by tumors.[1,2] In the primary site of tumor patients, upon coming into contact with the invasive tumor cells, extracellular matrix (ECM) components can be dissolved by proteolytic enzymes that are released by invasive tumor cells,[3,4] resulting in local defects of the basement membrane. Tumor cells can thus enter the blood lymphocyte circulation for distant spreading.[5] Therefore, impaired integrity of the basement membrane has been identified as an important histological marker of carcinoma invasiveness.[6] Since the invasive property of tumor cells is apparently the first stage of distant metastasis,[7] investigating the invasive capability by profiling the ECM degradation will be the priority assay, which will enable the early diagnosis and treatment of malignant tumors.[8,9]

Presently, the methods to measure the invasive cellular process can be carried out in vitro.[10,11] The trans-well assay by using the Matrigel-coated culture chambers is the most commonly used method, which observes cell migration through pores in an ECM filter under an optical microscope.[12] The method is widely accepted because it has a good imitation of the extracellular matrix environment and can reflect invasive capability.[13] However, there are also some inherent limitations. First, the trans-well assay is an end-point assay. Cell invasive capability is assessed by the final number of cells transferring across the EMC filter membrane. Cell invasive properties (e.g., cell behaviors, phenotypic diversity) cannot be recorded in this way. In addition, the less invasive cell cannot even be evaluated. Second, the pore size and height of the microscopic membrane filter in the trans-well assay may influence cell transport, and the action of gravity acting on the vertical up-and-down movement may affect the invasion performance.[14,15] Third, the transferring cells need dye labels for counting under the optical microscope, making the trans-well assay labor-intensive and time-consuming.[16] Therefore, establishing an effective and rapid assay method for evaluation of the cell invasion process is still an existing challenge and can be quite beneficial to tumor metastasis studies.

For developing function-oriented biochemical analytical methods, nanochannels have gained great interest in recent years.[17−21] A porous anodic alumina (PAA) membrane that

Received: January 19, 2021
Accepted: March 25, 2021
Published: April 9, 2021

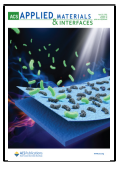

Scheme 1. Schematic Diagram of the Artificial ECM Degradation Model (EDM) Used for Dynamic Monitoring of Tumor Cell Invasive Capability

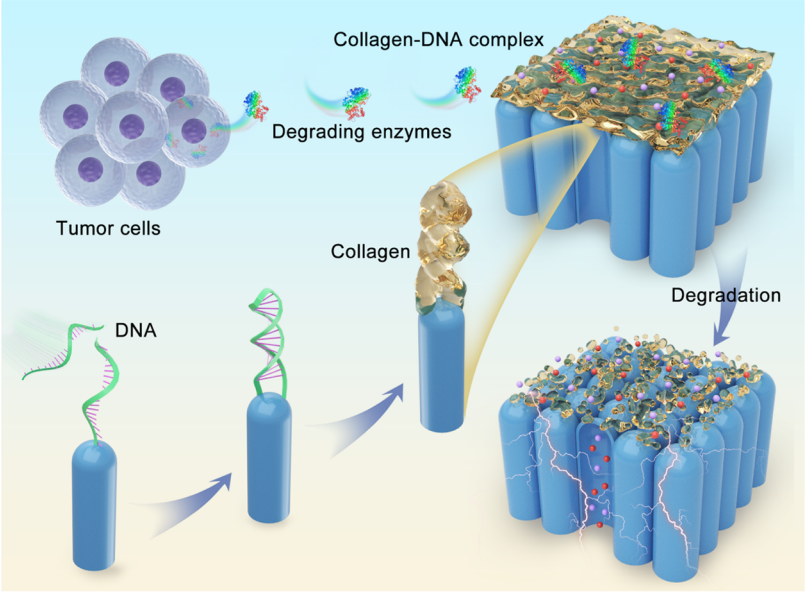

possesses an adjustable pore diameter, a good nanochannel array, and commercial availability opens a new avenue for developing highly sensitive sensors.[22−24] Most importantly, nanochannels in PAA not only provide a platform allowing signal amplification by several orders of magnitude but also reduce the background noise of the electrochemical detection, leading to good detection accuracy.[25] The ion transport in the nanochannels between two reservoirs is influenced by molecular volume, geometry, or charge property changes,[26−28] quickly reflected by a current change. Therefore, a combination of ECM degradation and electrochemical nanochannel detection is particularly appropriate for sensitive, rapid, and label-free detection of cell invasiveness.

Herein, by simulating the extracellular matrix, a bioinspired ECM degradation model (EDM) matrix has been designed and fabricated on PAA and thoroughly addressed in this work, with an ultimate objective to be used as the electrochemical trans-channel assay of the invasive capability of tumor cells. The EDM, self-assembled collagen−DNA complex gel, can be formed through electrostatic interaction and hydrogen-bond interaction on the barrier layer of the PAA membrane.[29−31] The degrading enzymes secreted by the tumor cells can digest the collagen;[32,33] thus, the steric hindrance is reduced significantly to allow ion transportation across the channels. Eventually, the ion current can be quantitatively and dynamically recorded for carrying out the invasive process of tumor cells, as shown in Scheme 1. In this design, the distinctive structure of the asymmetrical PAA membrane may provide a larger area for EDM modification,[34] and the narrow channel allows smaller steric hindrance to ion current response, which will significantly enlarge the detecting signal. Hence, compared to the trans-well assay, the electrochemical trans-channel assay can be carried out in a short period of time with more sensitive quantification. The invasive process and less invasive cells can be simultaneously monitored in our trans-channel assay. Thus, in virtue of the electrochemical technique, an efficient and label-free method has been proposed not only for the dynamic recording of the invasive behavior of the tumor cell but also for screening drugs that inhibit cell invasion and potentially prevent metastatic malignancy.

2. EXPERIMENTAL SECTION

2.1. Materials and Reagents. Collagen-like peptide (GPQGIFGQIGPQGIFGQIGPQGIFGQIGPQGIFGQ) designed as the optimal substrate for MMP-2 was synthesized by China Peptides Co., Ltd. The oligonucleotides DNA S1, 5′-CHO-$(CH_2)_6$-CAC GAC GTT GTA AAA CGA CGG CCA GAG CAG-3′, and its complementary strand DNA S2, 5′-CTG CTC TGG CCG TCG TTT TAC AAC-3′, were ordered from Sangon Biotech Co., Ltd. (Shanghai, China). Recombinant Human MMP-2 was purchased from Sino Biological, Inc., captopril, and 4-aminophenylmercuric acetate (APMA) were obtained from Genmed Scientifics, Inc. Crystal violet staining solution was obtained from Solarbio Technology Co., Ltd. MMP-2 from cell suspension was extracted and quantified with a Human MMP-2 ELISA kit from Beyotime Biotechnology Co., Ltd. (Shanghai, China); 24-well inserts used in the trans-well assay were purchased from Corning Co., Ltd. Potassium chloride (KCl) was obtained from Nanjing Chemical Reagent CO., Ltd (Nanjing, China). (3-Aminopropyl)trieoxysilane (APTES) and other certified analytical-grade reagents were purchased from Sigma-Aldrich (Shanghai, China). The porous anodic alumina (PAA) film was ordered from Hefei Puyuan Nanotechnology Co., Ltd (Anhui, China). All solutions were prepared with deionized water that had been purified with a Milli-Q purification system (Bedford, MA) to a resistance of 18.2 MΩ cm.

2.2. Instrumentation. Surface and flank morphologies of the PAA membrane were determined with a scanning electron microscope (SEM, SU8020, Japan) and an atomic force microscope (AFM, Bruker, Germany). To characterize the modification process of the probe, X-ray photoelectron spectroscope (XPS, ESCALAB 250XI, Thermo Fisher Scientific) was used to measure the X-ray photoelectron spectroscopy (XPS) spectra of the reactants at each step to verify the gradual modification of the PAA membrane. Ion currents were recorded by an electrochemical workstation (CHI 660D, Chenhua, China).

2.3. Collagen−DNA Complex Modification. PAA films were sequentially washed by ultrasonication in alcohol and water for 5 min to remove impurities in the nanochannel. They were dried with nitrogen and then placed in an ethanol solution containing 5% (3-aminopropyl)triethoxysilane (APTES) and shaken gently on a shaking table at room temperature for 12 h to graft the aminopropyl

https://doi.org/10.1021/acsami.1c01236
ACS Appl. Mater. Interfaces 2021, 13, 17268−17275

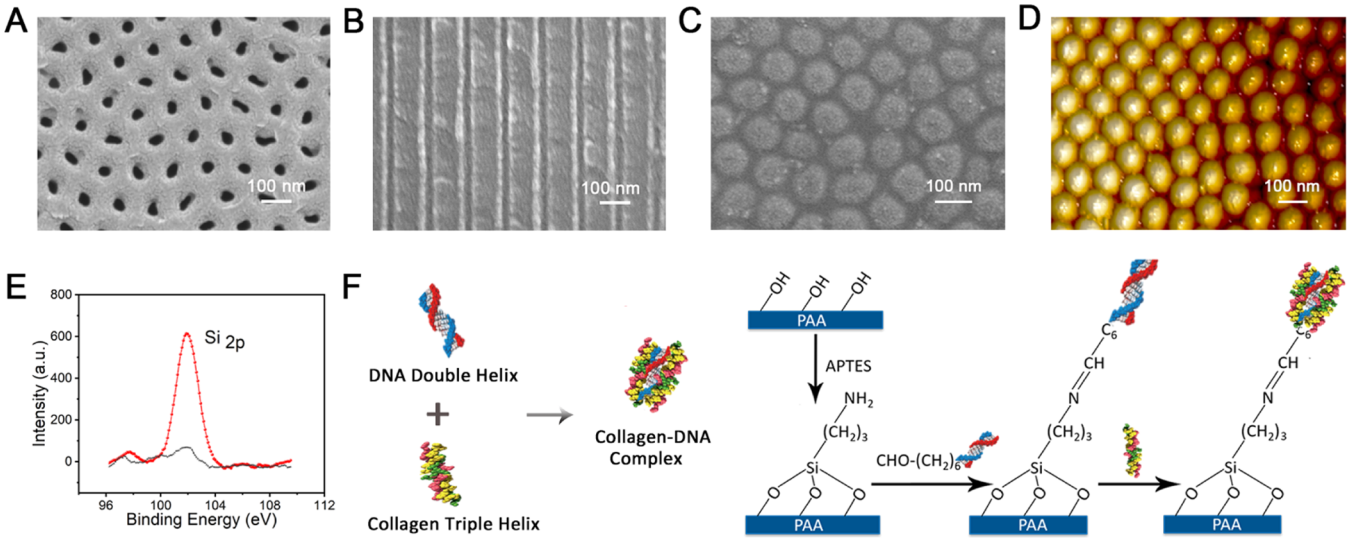

Figure 1. Assembly and characterizations of EDM on the PAA membrane. (A) Porous layer, (B) flank, and (C) barrier layer of the PAA membrane under a scanning electron microscope (SEM). (D) Barrier layer of the PAA membrane observed under an AFM. (E) Characterization of EDM by elemental analysis of Si 2p using X-ray photoelectron spectroscopy (XPS). (F) Schematic illustration of the fabrication process of the EDM.

functional groups. The PAA films were rinsed again with alcohol to remove the residual silylation reagent and dried with nitrogen, followed by baking at 120 °C for 1 h to cross-link the silane layer. DNA S1 solution was then dripped onto the porous layer side of the PAA membrane and reacted at room temperature for 24 h. It is important to note that a little water is added to the sealed culture dish to prevent evaporation of the DNA solution. Then, the PAA membrane was cleaned with ultrapure water to remove the free DNA S1. The DNA S2 strand was added to be paired with DNA S1 at 37 °C for 1 h to form a DNA double-stranded complex on the surface of PAA. Finally, 20 μL of 50 μM collagen buffer was dripped onto the surface of the double-stranded DNA-modified PAA membrane and reacted at 37 °C for 30 min so that collagen and DNA could self-assemble into a collagen−DNA complex through electrostatic interaction.

2.4. Electrochemical Detection of MMP-2 Activity. The pre-enzyme of MMP-2 was inactive and needed to be activated overnight at 37 °C with 1 mM APMA activator. The activated MMP-2 was diluted with TCNB to different concentrations for the next use. The modified collagen−DNA−PAA membrane and two electrolytic cells were fixed with a silicone gasket to prevent liquid leakage, and the two electrolytic cells were fixed together with metal clips. Cells were treated with 1 mM captopril at 37 °C for 24 h to assess the inhibition effect on MMP-2. Each experiment was performed in triplicate, and the gels were analyzed using semiquantitative densitometry; 1.5 mL of 10 mM KCl solution and 13.5 mL of 1× TCNB buffer (10 mM $CaCl_2$, 150 mM NaCl, and 50 mM Tris-HCl buffer containing 0.05% Brig) were added to each cell. Two Ag/AgCl reference electrodes full of a saturated potassium chloride solution were inserted into the cells to form a complete electrical circuit with the electrochemical workstation. MMP-2 (10 μL) with different concentrations was added on the porous layer side of the modified PAA membrane and incubated at 37 °C for 20 min. Current−voltage (I−V) characteristics between −1.0 and + 1.0 V adopting the technique of linear sweep voltammetry (LSV) were recorded by the electrochemical workstation at 37 °C.

2.5. Cell Invasion Assay. The cell invasion assay was performed by Matrigel-coated trans-well cell culture chambers (8 μm pore size). The 10.9 mg/mL Matrigel was diluted to 300 μg/mL by serum-free cell culture medium or phosphate-buffered saline (PBS) solution at 4 °C, and 100 μL of diluent was evenly added to the surface of a polycarbonate film in the upper chamber. It was placed in a cell incubator for 4 h to facilitate Matrigel polymerization, and then put in a superclean bench overnight. After removing serum for starvation for 12 h, well-grown cells were washed with PBS, digested with trypsin, and then washed with PBS 1−2 times. The suspended cells were cultured in serum-free medium containing 1% bovine serum albumin (BSA), and the cell density was adjusted to 0.5−10 × 10^5/mL. Medium (600 μL) containing 10% fetal bovine serum (FBS) was generally added to the lower chambers of the 24-well plate; 300 μL of cell suspension was added to the upper chambers. Finally, the cells were cultured in a humidified atmosphere (5% CO_2) at 37 °C for 6−48 h.

The Matrigel and the cells in the chambers were wiped gently with a cotton swab after medium removal. A new 24-well plate was added with 600 μL of 70% methanol solution, and these chambers were fixed for 30−60 min. Next, the methanol solution was discarded, and the chambers were stained with 0.1% crystal violet for 10−20 min and washed with PBS three times to remove the residual crystal violet. The upper side of the chamber was gently wiped with cotton swabs, and the dye that was not specifically bound to the upper surface of the chamber was erased for subsequent microscopic examination. After being properly air-dried, the cells were observed and counted from the field of a high-resolution microscope with upper, lower, left, middle, and right views.

2.6. Electrochemical Detection of MMP-2 Secreted by Cells. The cancer cells used in the experiments were MCF-7 cells. MCF-10A cells were analyzed for the control experiments. The MMP-2 in the cell culture medium supernatant was determined with the Human MMP-2 ELISA kit; 10 μL of the culture medium supernatant with different measured MMP-2 concentrations from cells was added to the porous layer side of the modified PAA membrane and incubated at 37 °C for 20 min. The electrochemical detection experiments were conducted using the methods mentioned above.

3. RESULTS AND DISCUSSION

3.1. Characterization of the PAA Membrane and Fabrication of the EDM. To get a clear observation of the microstructure of the EDM assembly, we have characterized the PAA membrane with a scanning electron microscope (SEM). Figure 1A shows the porous layer of the PAA membrane. The diameter of the channels is about 50 nm. The nanochannels that extend straight out are shown in Figure 1B. The barrier layer is clearly presented in the SEM image (Figure 1C) and the AFM image (Figure 1D), while there exist subnanometer channels within arrays of protuberances that allow ion transport to generate a current signal. With the well-

https://doi.org/10.1021/acsami.1c01236
ACS Appl. Mater. Interfaces 2021, 13, 17268−17275

organized channel array, a small steric hindrance change can trigger a significant electrochemical signal response, which allows a sensitive response after EDM assembly. After morphological characterization of the bare PAA membrane, we have then fabricated the EDM. The functionalization manifestation has been proceeded by means of X-ray photoelectron spectroscopy (XPS). The XPS spectrum of the (3-aminopropyl)trieoxysilane (APTES)-functionalized PAA membrane (red curve) presents an obvious Si 2p peak compared to that of the bare PAA membrane (gray curve), shown in Figure 1F, revealing successful modification of APTES, followed by a gradual modification of DNA and collagen, as illustrated in Figure 1F. Specified XPS tests for P 2p, C 1s, and N 1s have verified the modification (Figures S1 and S2). For the amino-activated PAA membrane, an obvious N 1s peak is observed (red curve), together with a corresponding increase in the C 1s peak value. Blue and green curves represent the PAA membrane modified with DNA and peptide, and the nitrogenous bases in DNA and amino acids in peptides both lead to an increase of the N 1s peak, respectively. Laser scanning confocal microscopy has also been adopted for the examination of DNA immobilization (Figure S3). Therefore, successful modifications of APTES, DNA, and peptide on the barrier of the PAA membrane have been manifested.

3.2. Sensing of Cell Invasion by the Trans-Channel Assay. The trans-channel assay property has been characterized by $I-V$ measurement in a home-made H-type electrolytic tank inserted with two Ag/AgCl reference electrodes (Figure 2A). Linear sweep voltammetry (LSV) has been adopted to record the current characteristics between −1 and +1 V over time. The collagen-like peptide used in the work is negatively charged like DNA, so the surface charge changes slightly. However, as shown in Figure S4, after the assembly of the collagen−DNA complex gel as the EDM, the current value at - 1 V decreases because the ion-transfer behavior is obstructed due to the steric hindrance. It has been observed that the current value reverses back after the cleavage of MMP-2; therefore, the enzyme digestion process can be reflected by the current signals. We have then conducted the experiments using PAA membranes with three pore sizes, 50, 90, and 200 nm, to study the influence of the diameter of the PAA membrane. Experimental results reveal that there is no obvious difference among the three groups as shown in Figure S5. The complex gel assembles after the modification of DNA on the PAA membrane, so DNA concentration may be of great importance in the performance of the EDM assay; thus, it has been investigated so as to achieve efficient assay conditions (Figure S6). To be clear, we denote the current drop value as the difference of the current value before and after the cleavage of the collagen−DNA complex modified on the PAA membrane by MMP-2. The current drop value increases sharply at the beginning when the DNA concentration increases from 1 to 20 μM and then levels off at higher concentrations, which indicates that 20 μM DNA can sufficiently accommodate the collagen peptides. Moreover, the effect of cell density on the assay has been explored to widen the detection range, as shown in Figure 2B,C. The current rises with increased cell density, which may contain more secreted enzymes.

3.3. Feasibility Investigation. The property of EDM for the cell invasiveness assay has also been additionally supported by the AFM imaging data. The collagen-like peptide on the

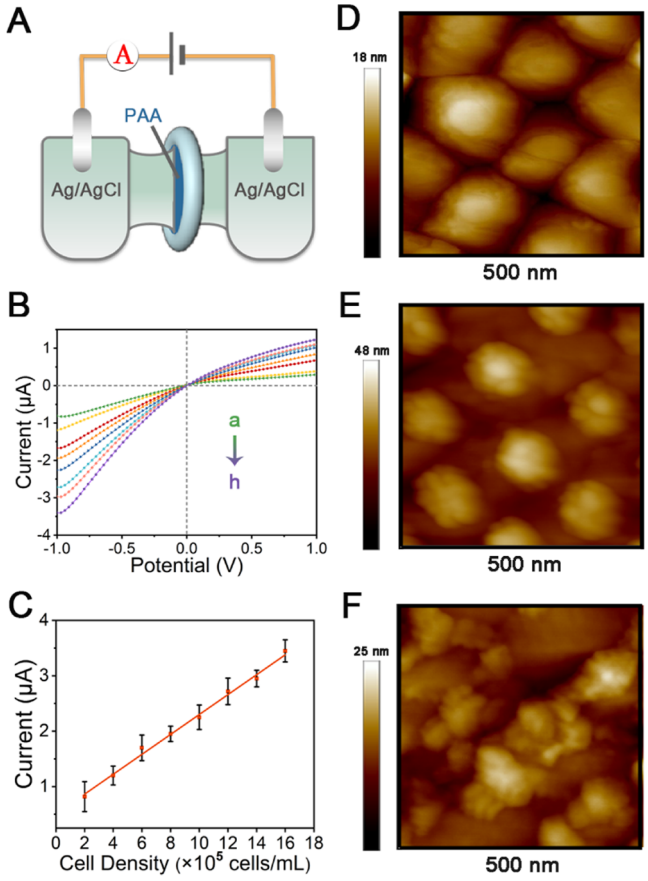

Figure 2. Electrochemical and AFM characterizations of the trans-channel device. (A) Schematic illustration of the electrochemical device. (B) $I-V$ curves of the EDM measured between −1 and + 1 V in response to different cell densities (a: 2×10^5, b: 4×10^5, c: 6×10^5, d: 8×10^5, e: 10×10^5, f: 12×10^5, g: 14×10^5, h: 16×10^5 cells/mL) and (C) linear calibration plot of the corresponding current values at −1 V vs the cell density. AFM image of the (D) bare PAA membrane and the collagen−DNA complex gel-modified PAA membrane (E) before and (F) after the incubation with cell culture medium. The electrolyte is 1.5 mL of 10 mM KCl solution and 13.5 mL of 1 × TCNB buffer. The cells used in the experiment are MCF-7 cells.

PAA membrane appears as an ordered assembly (Figure 2E), which covers the original morphology (Figure 2D). After addition of the cell culture medium that contains lyases like MMP-2, the morphological disorder and decreased thickness reveal that the proteolysis occurred after the incubation with cell culture medium (Figure 2F). In addition, the control experiment has also been conducted using the MCF-10A cells, and Figure S7 shows that the current of the collagen−DNA-modified PAA membrane does not change much before and after incubation with the noncancerous cell medium. Since MMPs are the only proteases involved in the invasion of cancer cells through the basement membrane, which is a thin and dense sheetlike structure,[35] fabricating a biomimetic EDM based on the assembly of collagen-like peptide on the PAA membrane for the detection of cell invasive capability is feasible.

3.4. Trans-Well Assay Validation and Advantages of the Trans-Channel Assay. For monitoring of the cell invasive capability, the $I-V$ properties of the EDM at different incubation time points under optimized conditions have then

https://doi.org/10.1021/acsami.1c01236
ACS Appl. Mater. Interfaces 2021, 13, 17268−17275

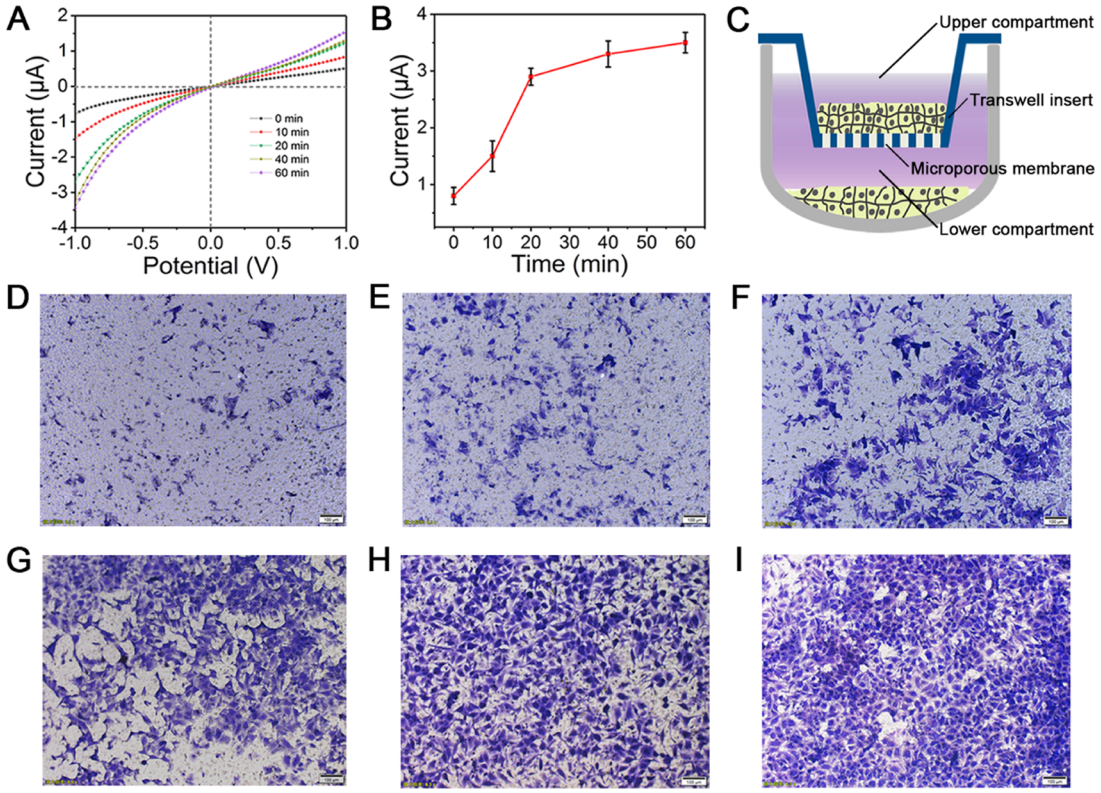

Figure 3. Comparison between the electrochemical trans-channel assay and the trans-well assay. (A) *I*−*V* properties of the EDM between −1 and +1 V at different time points. (B) Current values at −1 V vs different enzyme digestion times. (C) Diagram of the trans-well insert apparatus used to measure cell invasion. (D−I) Representative pictures of cell invasion at the time periods of 18, 24, 30, 36, 42, and 48 h, respectively. The electrolyte is 1.5 mL of 10 mM KCl solution and 13.5 mL of 1× TCNB buffer. The cells used in the experiment are MCF-7 cells.

been explored by adopting the LSV electrochemical technique between −1 and +1 V (Figure 3A). The dots in Figure 3B represent the current value at −1 V. They show an increasing trend and a big rise in the first 20 min, which indicates that the ECM degradation is in progress in the device. Since the trans-well assay is the standard tool for studying matrix invasion,[36,37] the cell invasive capability along with incubation time has been investigated by the trans-well cell invasion assay as a validation.[38] Two culture compartments are separated by a microporous membrane filter as shown in Figure 3C. Cell suspension has been added on top of the trans-well membrane in the upper chamber and culture solution has been added to the lower chamber. Cell migration has been performed according to the procedures described in the Experimental section. Representative pictures of cell invasion at the time of 18, 24, 30, 36, 42, and 48 h (Figure 3D−I) indicate the same rising tendency with our method, but the time needed for the test in our method is significantly reduced. Therefore, this proves that our trans-channel assay method is well qualified to detect cell invasiveness, avoiding the influences of the microporous membrane pore size and gravity, overcoming inevitable shortcomings in the trans-well assay. It is clear that the electrochemical EDM invasion assay also shows the merit of rapid and dynamic monitoring, which is much superior to the end-point determination in the trans-well assay.

3.5. Evaluation of the Tumor Cell Invasiveness. For proof of concept, MMP-2 secreted by the invasive tumor cells[39] has been further used to examine the electrochemical response of EDM. The effects of cell concentration or the MMP-2 concentration in cell culture medium on cell invasion have thus been tested. Different cell concentrations, 0.5, 1.0, 1.5, 2.0, and 2.5 × 10^5/mL, are chosen as the experimental concentrations to conduct the trans-well assay. Microscopic images are captured at 42 h as shown in Figure S8A−E that the number of cells that travel to the lower chamber is found to increase with the increase of the cell concentrations that are added to the upper compartment. To be in parallel with the trans-well assay, our EDM-based electrochemical tests have been carried out. Figure 4A shows the *I*−*V* responses of the EDM under different concentrations of MMP-2, and Figure 4B shows the corresponding current drop values. It is easy to see that there is a correlation between the current drop value and

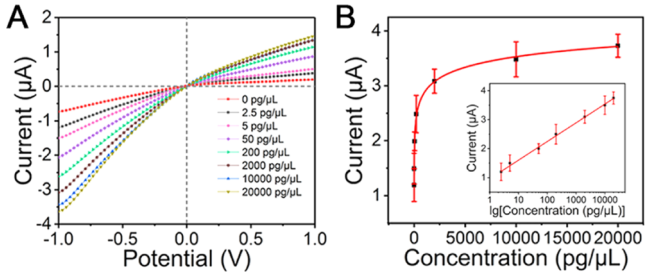

Figure 4. (A) *I*−*V* responses of the EDM-modified PAA with different concentrations of MMP-2 contained in the cell culture medium. (B) Corresponding current drop values of the EDM at −1 V vs cell culture medium containing different concentrations of MMP-2; inset: linear calibration plot of current values recorded at −1 V vs the logarithm of different MMP-2 concentrations. The electrolyte is 1.5 mL of 10 mM KCl solution and 13.5 mL of 1× TCNB buffer. The cells used in the experiment are MCF-7 cells.

https://doi.org/10.1021/acsami.1c01236
ACS Appl. Mater. Interfaces 2021, 13, 17268−17275

the concentration of MMP-2 in cell culture medium. As the MMP-2 concentration increases, the EDM gets broken more efficiently, which can be reflected by the quick increase in the electrochemical signal.

3.6. Specificity, Stability, and Application of the Trans-Channel Assay. The specificity of the EDM-based electrochemical assay has been examined through incubation with potential interference species as shown in Figure 5A.

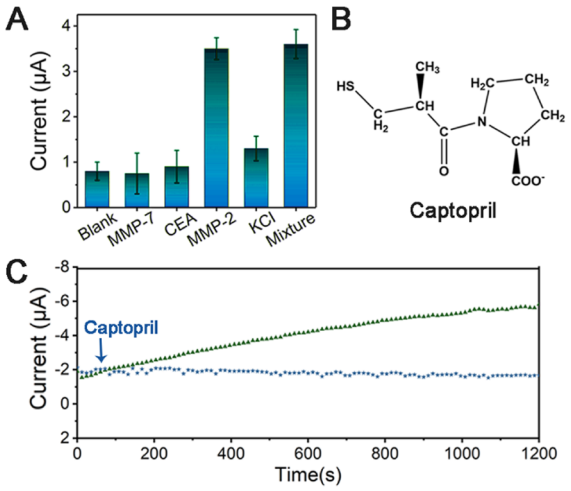

Figure 5. Specificity validation and application of the EDM. (A) Current drop values of the EDM at −1 V vs different incubation systems. (B) Chemical structure of captopril. (C) Current of the EDM assay with or without the inhibitory effect of captopril. The electrolyte is 1.5 mL of 10 mM KCl solution and 13.5 mL of 1× TCNB buffer. The cells used in the experiment are MCF-7 cells.

Results show that there are apparent current changes in the systems of the MMP-2 enzyme solution and the mixture containing MMP-2, confirming that the collagen modified on the PAA membrane in this work can be specifically cleaved by MMP-2. Therefore, an EDM simulating the ECM degradation has been created for evaluation of the premetastatic tumor cells. After the collagen degradation in the first round of the experiment, the used PAA membrane has been modified again with the collagen to study cycling performance. As shown in Figure S9, the interaction of this EDM is reversible, so the membrane can be reused after one test, though with little performance decline. In addition, the EDM has been used to examine the inhibitory effect of captopril on MMP activity, whose chemical structure is shown in Figure 5B. Optimization of the concentration of captopril has been conducted (Figure S10), and the current−time (I−t) curves have been adopted to make a comparison (Figure 5C).[40] The green curve represents the normal EDM assay and the current changes along with the collagen−DNA degradation. Captopril directly inhibits MMP-2 activity and impacts tumor invasion and migration,[41] and the effect is well demonstrated in the EDM assay. The blue five-pointed stars curve shows no growth, which indicates the possibility that the EDM could be used for inhibitor screening.

CONCLUSIONS

This study has demonstrated an electrochemical trans-channel assay for tumor cell invasiveness with simplicity and sensitivity. Based on biomimetic EDM, the modification of the collagen−DNA complex on the PAA membrane, MMP-2 contained in the cell culture medium degrades the collagen, which significantly increases the current response of the nanochannel. The in situ degradation has a natural advantage of dynamic monitoring of the cell invasive capability, which overcomes the complex operation steps in the currently used trans-well assay. Owing to the sensitive response of EDM and the fast response of the trans-channel ionic signals, the assay can be accomplished within 20 min with high sensitivity. In addition, as a sensitive assay of tumor cell invasiveness, the EDM-based electrochemical assay has shown great potential in developing a reliable and convenient analytical platform for the dynamic analysis of cellular response to certain challenges such as drug screening and treatment.

ASSOCIATED CONTENT

Supporting Information

The Supporting Information is available free of charge at https://pubs.acs.org/doi/10.1021/acsami.1c01236.

AFM image of the PAA membrane; XPS spectra of the bare and modified PAA membranes; element ratios; laser scanning confocal microscopy (LSCM) characterizations of the PAA membranes; I−V responses recording cancer and noncancerous cell invasion; optimization of the diameter of the PAA channel, DNA concentration, and captopril concentration; and representative pictures of cell invasion with cell concentration (PDF)

AUTHOR INFORMATION

Corresponding Authors

Tao Gao − *Jiangsu Key Laboratory for Molecular and Medical Biotechnology, College of Life Sciences, Nanjing Normal University, Nanjing 210023, P. R. China;* orcid.org/0000-0002-3687-8945; Email: taogao@njnu.edu.cn

Farid A. Harraz − *Promising Centre for Sensors and Electronic Devices (PCSED), Advanced Materials and Nano-Research Centre, Najran University, Najran 11001, Saudi Arabia; Nanomaterials and Nanotechnology Department, Central Metallurgical Research and Development Institute (CMRDI), Cairo 11421, Egypt*; Email: faharraz@nu.edu.sa

Genxi Li − *State Key Laboratory of Pharmaceutical Biotechnology, School of Life Sciences, Nanjing University, Nanjing 210023, P. R. China; Center for Molecular Recognition and Biosensing, School of Life Sciences, Shanghai University, Shanghai 200444, P. R. China;* orcid.org/0000-0001-9663-9914; Email: genxili@nju.edu.cn

Authors

Liu Shi − *State Key Laboratory of Pharmaceutical Biotechnology, School of Life Sciences, Nanjing University, Nanjing 210023, P. R. China*

Lin Wang − *State Key Laboratory of Pharmaceutical Biotechnology, School of Life Sciences, Nanjing University, Nanjing 210023, P. R. China*

Xuemei Ma − *State Key Laboratory of Pharmaceutical Biotechnology, School of Life Sciences, Nanjing University, Nanjing 210023, P. R. China*

Mohammed Jalalah − *Promising Centre for Sensors and Electronic Devices (PCSED), Advanced Materials and Nano-Research Centre and Department of Electrical Engineering, Faculty of Engineering, Najran University, Najran 11001, Saudi Arabia;* orcid.org/0000-0002-6828-3874

https://doi.org/10.1021/acsami.1c01236
ACS Appl. Mater. Interfaces 2021, 13, 17268−17275

Saeed A. Alsareii − *Department of Surgery, College of Medicine, Najran University, Najran, Saudi Arabia*

Complete contact information is available at: https://pubs.acs.org/10.1021/acsami.1c01236

Author Contributions

This manuscript was written through contributions of all authors. L.S. and G.L. conceived the projects. L.S., L.W., X.M., and T.G. designed and performed the experiments and collected the data. L.S., M.J., S.A.A., and F.A.H. analyzed and discussed the data. All authors discussed the results and contributed to the writing of this manuscript. All authors have given approval to the final version of the manuscript.

Notes

The authors declare no competing financial interest.

■ ACKNOWLEDGMENTS

The authors extend their appreciation to the Deputyship for Research & Innovation, Ministry of Education, Saudi Arabia, for funding this research work through project number 875, and the support of the National Natural Science Foundation of China (grant no. 81772593), the Natural Science Foundation of Jiangsu Province (grant no. BK20190693), and the Research and Innovation Project for College Graduates of Jiangsu Province (grant no. KYCX20_0033).

■ REFERENCES

(1) Swaminathan, V.; Mythreye, K.; Obrien, E. T.; Berchuck, A.; Blobe, G. C.; Superfine, R. J. C. R. Mechanical Stiffness Grades Metastatic Potential in Patient Tumor Cells and in Cancer Cell Lines. *Cancer Res.* **2011**, *71*, 5075−5080.

(2) Hanahan, D.; Weinberg, R. A. The Hallmarks of Cancer. *Cell* **2000**, *100*, 57−70.

(3) Matsumura, S.-i.; Iwanaga, S.; Mochizuki, S.; Okamoto, H.; Ogawa, S.; Okada, Y. Targeted Deletion or Pharmacological Inhibition of MMP-2 Prevents Cardiac Rupture after Myocardial Infarction in Mice. *J. Clin. Invest.* **2005**, *115*, 599−609.

(4) Kessenbrock, K.; Plaks, V.; Werb, Z. J. C. Matrix Metalloproteinases: Regulators of the Tumor Microenvironment. *Cell* **2010**, *141*, 52−67.

(5) Kurz, A. R. M.; Pruenster, M.; Rohwedder, I.; Ramadass, M.; Schäfer, K.; Harrison, U.; Gouveia, G.; Nussbaum, C.; Immler, R.; Wiessner, J. R.; Margraf, A.; Lim, D.-S.; Walzog, B.; Dietzel, S.; Moser, M.; Klein, C.; Vestweber, D.; Haas, R.; Catz, S. D.; Sperandio, M. MST1-Dependent Vesicle Trafficking Regulates Neutrophil Transmigration through the Vascular Basement Membrane. *J. Clin. Invest.* **2016**, *126*, 4125−4139.

(6) Veidal, S. S.; Karsdal, M. A.; Nawrocki, A.; Larsen, M. R.; Dai, Y.; Zheng, Q.; Hägglund, P.; Vainer, B.; Skjøt-Arkil, H.; Leeming, D. J. Assessment of Proteolytic Degradation of the Basement Membrane: a Fragment of Type IV Collagen as a Biochemical Marker for Liver Fibrosis. *Fibrog. Tissue Repair* **2011**, *4*, No. 22.

(7) Hanahan, D.; Weinberg, R. A. J. C. Hallmarks of Cancer: The Next Generation. *Cell* **2011**, *144*, 646−674.

(8) Artym, V. V.; Yamada, K. M.; Mueller, S. C. *Extracellular Matrix Protocols*, 2nd ed.; Even-Ram, S.; Artym, V., Eds.; Humana Press: Totowa, NJ, 2009; pp 211−219.

(9) Li, R.; Ma, Y.; Zhao, M.; Hu, Z.; Wei, Z. J. A. C. Device to Study the Cell Invasion Behavior and Phenotypic Profile at Single Cell Level. *Anal. Chem.* **2018**, *90*, 1691−1700.

(10) Ma, L.; Teruya-Feldstein, J.; Weinberg, R. A. Tumour Invasion and Metastasis Initiated by MicroRNA-10b in Breast Cancer. *Nature* **2007**, *449*, 682−688.

(11) Sahai, E.; Marshall, C. J. Differing Modes of Tumour Cell Invasion have Distinct Requirements for Rho/ROCK Signalling and Extracellular Proteolysis. *Nat. Cell Biol.* **2003**, *5*, 711−719.

(12) Chaw, K. C.; Manimaran, M.; Tay, F. E. H.; Swaminathan, S. Matrigel Coated Polydimethylsiloxane Based Microfluidic Devices for Studying Metastatic and Non-metastatic Cancer Cell invasion and migration. *Biomed. Microdevices* **2007**, *9*, 597−602.

(13) Maria, O. M.; Maria, O.; Liu, Y.; Komarova, S. V.; Tran, S. D. Matrigel Improves Functional Properties of Human Submandibular Salivary Gland Cell Line. *Int. J. Biochem. Cell* **2011**, *43*, 622−631.

(14) Wolf, K.; Te Lindert, M.; Krause, M.; Alexander, S.; Te Riet, J.; Willis, A. L.; Hoffman, R. M.; Figdor, C. G.; Weiss, S. J.; Friedl, P. Physical Limits of Cell Migration: Control by ECM Space and Nuclear Deformation and Tuning by Proteolysis and Traction Force. *J Cell Biol.* **2013**, *201*, 1069−1084.

(15) Lei, K. F.; Tseng, H.-P.; Lee, C.-Y.; Tsang, N.-M. Quantitative Study of Cell Invasion Process under Extracellular Stimulation of Cytokine in a Microfluidic Device. *Sci. Rep.* **2016**, *6*, No. 25557.

(16) Weiger, M. C.; Vedham, V.; Stuelten, C. H.; Shou, K.; Herrera, M.; Sato, M.; Losert, W.; Parent, C. A. Real-time Motion Analysis Reveals Cell Directionality as an Indicator of Breast Cancer Progression. *PLoS One* **2013**, *8*, No. e58859.

(17) Liu, J.; Fu, B.; Zhang, Z. Ionic Current Rectification Triggered Photoelectrochemical Chiral Sensing Platform for Recognition of Amino Acid Enantiomers on Self-Standing Nanochannel Arrays. *Anal. Chem.* **2020**, *92*, 8670−8674.

(18) Li, M.; Xiong, Y.; Lu, W.; Wang, X.; Liu, Y.; Na, B.; Qin, H.; Tang, M.; Qin, H.; Ye, M.; Liang, X.; Qing, G. Functional Nanochannels for Sensing Tyrosine Phosphorylation. *J. Am. Chem. Soc.* **2020**, *142*, 16324−16333.

(19) Jiao, S.; Liu, L.; Wang, J.; Ma, K.; Lv, J. A Novel Biosensor Based on Molybdenum Disulfide (MoS2) Modified Porous Anodic Aluminum Oxide Nanochannels for Ultrasensitive microRNA-155 Detection. *Small* **2020**, *16*, No. 2001223.

(20) Wang, J.; Hou, J.; Zhang, H.; Tian, Y.; Jiang, L. A Novel Biosensor Based on Molybdenum Disulfide (MoS2) Modified Porous Anodic Aluminum Oxide Nanochannels for Ultrasensitive MicroRNA-155 Detection. *ACS Appl. Mater. Interfaces* **2018**, *10*, 2033−2039.

(21) Zhang, Z.; Huang, X.; Qian, Y.; Chen, W.; Wen, L.; Jiang, L. Engineering Smart Nanofluidic Systems for Artificial Ion Channels and Ion Pumps: From Single-pore to Multichannel Membranes. *Adv. Mater.* **2020**, *32*, No. 1904351.

(22) Gao, H.; Sun, R.; He, L.; Qian, Z.-J.; Zhou, C.; Hong, P.; Sun, S.; Mo, R.; Li, C. In Situ Growth Visualization Nanochannel Membrane for Ultrasensitive Copper Ion Detection under the Electric Field Enrichment. *ACS Appl. Mater. Interfaces* **2020**, *12*, 4849−4858.

(23) Zhu, W.; Chen, Y.; He, Y.; Fang, W.; Ying, Y.; Li, Y.; Fu, Y. Cooperation Mode of Outer Surface and Inner Space of Nanochannel: Separation-Detection System Based on Integrated Nanochannel Electrode for Rapid and Facile Detection of Salmonella. *Anal. Chem.* **2020**, *92*, 1818−1825.

(24) Zhang, Q.; Kang, J.; Xie, Z.; Diao, X.; Liu, Z.; Zhai, J. Highly Efficient Gating of Electrically Actuated Nanochannels for Pulsatile Drug Delivery Stemming from a Reversible Wettability Switch. *Adv. Mater.* **2018**, *30*, No. 1703323.

(25) Wang, C.; Zhao, X.-P.; Liu, F.-F.; Chen, Y.; Xia, X.-H.; Li, J. Dendrimer-Au Nanoparticle Network Covered Alumina Membrane for Ion Rectification and Enhanced Bioanalysis. *Nano Lett.* **2020**, *20*, 1846−1854.

(26) Zhu, Z.; Wang, D.; Tian, Y.; Jiang, L. Ion/Molecule Transportation in Nanopores and Nanochannels: From Critical Principles to Diverse Functions. *J. Am. Chem. Soc.* **2019**, *141*, 8658−8669.

(27) Xie, G.; Li, P.; Zhao, Z.; Kong, X.-Y.; Zhang, Z.; Xiao, K.; Wang, H.; Wen, L.; Jiang, L. Bacteriorhodopsin-Inspired Light-Driven Artificial Molecule Motors for Transmembrane Mass Transportation. *Angew. Chem., Int. Ed.* **2018**, *57*, 16708−16712.

(28) Li, R.; Fan, X.; Liu, Z.; Zhai, J. Smart Bioinspired Nanochannels and their Applications in Energy-Conversion Systems. *Adv. Mater.* **2017**, *29*, No. 1702983.

(29) Mrevlishvili, G. M.; Svintradze, D. V. Complex between Triple Helix of Collagen and Double Helix of DNA in Aqueous Solution. *Int. J. Biol. Macromol.* **2005**, *35*, 243−245.
(30) Prasadh, S.; Wong, R. C. W. Unraveling the Mechanical Strength of Biomaterials Used as a Bone Scaffold in Oral and Maxillofacial Defects. *Int. J. Oral Sci.* **2018**, *15*, 48−55.
(31) Pidaparti, R. M.; Svintradze, D. V.; Shan, Y.; Yokota, H. Optimization of Hydrogen Bonds for Combined DNA/Collagen Complex. *J. Theor. Biol.* **2009**, *256*, 149−156.
(32) Jackson, S. R.; Eckford, S. D.; Abrams, P.; Avery, N. C.; Tarlton, J. F.; Bailey, A. J. Changes in Metabolism of Collagen in Genitourinary Prolapse. *Lancet* **1996**, *347*, 1658−1661.
(33) Galis, Z. S.; Sukhova, G. K.; Lark, M. W.; Libby, P. Increased Expression of Matrix Metalloproteinases and Matrix Degrading Activity in Vulnerable Regions of Human Atherosclerotic Plaques. *J Clin. Invest.* **1994**, *94*, 2493−2503.
(34) Shi, L.; Mu, C.; Gao, T.; Chai, W.; Sheng, A.; Chen, T.; Yang, J.; Zhu, X.; Li, G. Rhodopsin-Like Ionic Gate Fabricated with Graphene Oxide and Isomeric DNA Switch for Efficient Photocontrol of Ion Transport. *J. Am. Chem. Soc.* **2019**, *141*, 8239−8243.
(35) Hotary, K.; Li, X. Y.; Allen, E.; Stevens, S. L.; Weiss, S. J. A Cancer Cell Metalloprotease Triad Regulates the Basement Membrane Transmigration Program. *Genes Dev.* **2006**, *20*, 2673−2686.
(36) Sodek, K. L.; Brown, T. J.; Ringuette, M. J. Collagen I but not Matrigel Matrices Provide an MMP-Dependent Barrier to Ovarian Cancer Cell Penetration. *BMC Cancer* **2008**, *8*, No. 223.
(37) Nabha, S. M.; dos Santos, E. B.; Yamamoto, H. A.; Belizi, A.; Dong, Z.; Meng, H.; Saliganan, A.; Sabbota, A.; Bonfil, R. D.; Cher, M. L. Bone Marrow Stromal Cells Enhance Prostate Cancer Cell Invasion through Type I Collagen in an MMP-12 Dependent Manner. *Int. J. Cancer* **2008**, *122*, 2482−2490.
(38) Wang, Z.; Zou, Q.; Song, M.; Chen, J. NEAT1 Promotes Cell Proliferation and Invasion in Hepatocellular Carcinoma by Negative Regulating MiR-613 Expression. *Biomed. Pharmacother.* **2017**, *94*, 612−618.
(39) Davies, B.; Waxman, J.; Wasan, H.; Abel, P.; Williams, G.; Krausz, T.; Neal, D.; Thomas, D.; Hanby, A.; Balkwill, F. Levels of Matrix Metalloproteases in Bladder Cancer Correlate with Tumor Grade and Invasion. *Cancer Res.* **1993**, *53*, 5365−5369.
(40) Williams, R. N.; Parsons, S. L.; Morris, T. M.; Rowlands, B. J.; Watson, S. A. Inhibition of Matrix Metalloproteinase Activity and Growth of Gastric Adenocarcinoma Cells by an Angiotensin Converting Enzyme Inhibitor in In Vitro and Murine Models. *Eur. J. Surg. Oncol.* **2005**, *31*, 1042−1050.
(41) Prontera, C.; Mariani, B.; Rossi, C.; Poggi, A.; Rotilio, D. Inhibition of Gelatinase A (MMP-2) by Batimastat and Captopril Reduces Tumor Growth and Lung Metastases in Mice Bearing Lewis Lung Carcinoma. *Int. J. Cancer* **1999**, *81*, 761−766.

https://doi.org/10.1021/acsami.1c01236
ACS Appl. Mater. Interfaces 2021, 13, 17268−17275